논문 00-02-08

Regularized Modified Newton-Raphson Algorithm for Electrical Impedance Tomography Based on the Exponentially Weighted Least Square Criterion

전기 임피던스 단층촬영을 위한 지수적으로 가중된 최소자승법을 이용한 수정된 조정 Newton-Raphson 알고리즘

Kyung-Youn Kim*, Bong-Seok Kim*
(金 慶 淵*, 金 奉 奭*)

Abstract

In EIT(electrical impedance tomography), the internal resistivity(or conductivity) distribution of the unknown object is estimated using the boundary voltage data induced by different current patterns using various reconstruction algorithms. In this paper, we present a regularized modified Newton-Raphson(mNR) scheme which employs additional *a priori* information in the cost functional as soft constraint and the weighting matrices in the cost functional are selected based on the exponentially weighted least square criterion. The computer simulation for the 32 channels synthetic data shows that the reconstruction performance of the proposed scheme is improved compared to that of the conventional regularized mNR at the expense of slightly increased computational burden.

Keywords : Electrical impedance tomograph, Regularization method, Weighted least square criterion

요 약

전기 임피던스 단층촬영에서는, 각기 다른 주입 전류패턴에 의해 유기된 경계면의 전압 값을 이용하여 다양한 복원 알고리즘에 의해 물체의 내부 저항률(전도율) 분포를 추정한다. 본 논문에서는, 부가적인 사전 정보를 soft 제약조건으로 비용함수에 추가하고, 비용함수의 가중행렬을 지수적으로 가중된 최소자승법에 근거하여 선택하는 수정된 조정 Newton-Raphson(mNR) 법을 제안한다. 32채널에 대한 컴퓨터 시뮬레이션 결과, 제안된 방법은 기존의 조정 mNR 법에 비해 계산부담은 약간 증가하지만 복원성능이 개선됨을 보인다

* 濟州大學校 工科大學 電氣電子工學部.
(School of Electrical &Electronic Engineering, College of Engineering, Cheju National Univ.)
接受日: 2000年7月18日 修正完了日: 2000年11月9日

I. Introduction

EIT(electrical impedance tomography) plays an important role in monitoring tools for the process

engineering such as biomedical, geological and chemical engineering, due to its relatively cheap electronic hardware requirements and nonintrusive measurement properties [1-3]. In EIT different current patterns are injected to the unknown object through electrodes and the corresponding voltages are measured on its boundary surface. The physical relationship between inner resistivity(or conductivity) and boundary surface voltage is governed by the nonlinear Laplace equation with appropriate boundary conditions so that it is impossible to obtain the closed-form solution for the resistivity(or conductivity) distribution. Hence, the internal resistivity(or conductivity) distribution of the unknown object is estimated using the boundary voltage data based on various reconstruction algorithms.

Yorkey et al.[4] developed a modified Newton-Raphson(mNR) algorithm for static EIT image reconstruction and compared it with other existing algorithms such as backprojection, perturbation and double constraints methods. They concluded that the mNR reveals relatively good performance in terms of convergence rate and residual error compared to that of the other methods.

However, in real situations, the mNR method is often failed to obtain satisfactory images from physical data due to large modeling error, poor signal to noise ratios(SNRs) and ill-conditioned(ill-posed) characteristics. That is, the ratio between the maximum and minimum eigenvalues of the information matrix(or Hessian matrix) is very large. In particular, the ill-conditioning of the information matrix results in an inaccurate matrix inverse so that the resistivity(or conductivity) update process is very sensitive to the modeling and measurement errors.

To get around such ill-conditioned difficulties there have been various regularization approaches in the literature[5-11], but it still remains a great deal of debate. Basically, regularization methods have a smoothing effect on the iterative procedure, improving the conditioning of the information matrix. Among them, Murai et al.[5] used singular value decomposition(SVD) method and Akaikes information criterion[6] omitting very small eigenvalues of the Hessian matrix, therefore reducing the condition number of the Hessian matrix. Levenberg al.[7] introduced matrix coefficient method which has better reconstruction performance than the SVD method. More recently, Cohen-Bacrie et al.[8] suggested another regularization scheme using variance uniformization constraint. In addition, Tikhonov and subspace regularization techniques are employed by Vauhkonen et al.[9].

In this paper, we developed a regularized mNR algorithm for static EIT imaging based on the exponentially weighted least square criteria. The main idea of this paper is that the additional regularization constraint which incorporates *a priori* information into the object functional is helpful to stabilize the mNR reconstruction algorithm only in the transient convergence period. As the iterative solution converges to the real solution, the ill-conditioning problem becomes less severe. Therefore, in the steady state period, it is desirable to discard the additional constraint to avoid any distortion in final reconstructed image. To accomplish this purpose, exponential weighting matrices are employed to the objective functional, which are functions of the iteration number. Computer simulations for the 32-channel synthetic data are provided to illustrate the performance of the proposed algorithm.

II. Problem Formulation and reconstruction algorithm

2.1 Governing Equation

When electrical currents $I_l(l=1.2.....E)$ is injected into the object $\Omega \in R^{-1}$ through electrodes $e_l(l=1.2.....E)$ attached on the boundary $\partial\Omega$ and the

resistivity distribution $\rho(x,y)$ is known for the Ω, the corresponding induced electrical potential $u(x,y)$ can be determined uniquely from the nonlinear Laplace equation which can be derived from the Maxwell equation and Ohms law, and the Neumann type boundary condition as follows:

$$\nabla \cdot \rho^{-1} \nabla u = 0 \quad \text{in } \Omega \tag{1}$$

$$\int_{e_l} \rho^{-1} \frac{\partial u}{\partial n} dS = I_l \quad \text{on } e_l \ (l=1,2,...,E), \tag{2}$$

where, n is outward pointing normal vector. In addition, we have the following two conditions for the injected currents and measured voltages by taking into account the conservation of electrical charge and appropriate selection of ground electrode, respectively.

$$\sum_{l=1}^{E} I_l = 0 , \tag{3}$$

$$\sum_{l=1}^{E} V_l = 0 , \tag{4}$$

where, $V_l (l = 1.2.....E)$ are the induced voltages on the electrodes.

The computation of the potential $u(x,y)$ for the given resistivity distribution $\rho(x,y)$ and boundary condition I_l is called the forward problem. The numerical solution for the forward problem can be obtained using the finite element method(FEM). In the FEM, the object area is discretized into small elements having a node at each corner. It is assumed that the resistivity distribution is constant within an element. The potential at each node is calculated by discretizing the Eq. (1) into $Y\nu = c$, where $Y \in R^{N \times N}$ is so-called stiffness matrix and N is the numbers of FEM nodes. Y and c are the functions of the resistivity distribution and the injected current patterns, respectively.

2.2 A brief review of the conventional regularized mNR

To reconstruct the resistivity distribution inside the object, we have to solve the nonlinear ill-posed inverse problem. The regularization techniques are needed to obtain stable solutions due to the ill-posedness. The regularized cost functional to be minimized is written as follows:

$$\Phi(\rho_k) = \frac{1}{2}[\| V_o - f(\rho_k) \| + \alpha \| L\rho_k \|], \tag{5}$$

where, $V_o \in R^{EP \times 1}$ is stacked boundary measured voltage and E and P are the numbers of electrodes on the surface and injected current patterns, respectively. $\rho_k \in R^{M \times 1}$ is the resistivity distribution at the k-th iteration and M is the numbers of finite elements in FEM. In Eq. (5), $L \in R^{M \times M}$ and α are the regularization matrix and regularization parameter, respectively. There are many approaches in the literature[8-11] to construct L and α, but the usual choice is to fix $L = I_M$ and to adjust α empirically.

Then, the mNR-type resistivity update equation is given by the following iterative form as;

$$\rho_{k+1} = \rho_k + \Delta\rho_k , \tag{6}$$

where,

$$\Delta\rho_k = \{[f'(\rho_k)]^T f'(\rho_k) + \alpha L\}^{-1} \cdot \{[f'(\rho_k)]^T (V_o - f(\rho_k)) - \alpha L\rho_k\} . \tag{7}$$

In Eq. (7), $f'(\rho_k)$ stands for the Jacobian matrix which is defined by

$$[f'(\rho)]_{ij} \equiv \frac{\partial f_i}{\partial \rho_j} , \tag{8}$$

and the ill-conditioning of the information matrix is smoothed due to the regularization term.

2.3 The proposed regularized mNR scheme

The measurement equation can be described as the following nonlinear mapping with measurement error:

$$V_o = f(\rho_k) + w_k . \tag{9}$$

It is assumed that the measurement error w_k is white Gaussian noise with variance as:

$$E[w_k w_k^T] = R_k \tag{10}$$

An additional information about the resistivity distribution can be utilized as the soft constraint to improve the performance of the reconstruction algorithm.

$$L(\rho^* - \rho_k) = \mu_k , \tag{11}$$

where, $L \in R^{M \times M}$ is regularization matrix and ρ^* is *a priori* information about true resistivity distribution. In Eq. (11), μ_k represents the uncertainty in the physical adherence of the constraint. Also, it is assumed that the uncertainty μ_k is white Gaussian noise with variance as:

$$E[\mu_k \mu_k^T] = Q_k . \tag{12}$$

By taking into account Eqs. (9) and (11), the augmented cost functional including the soft constraint can be formulated in the exponentially weighted least square criteria as:

$$\Phi_a(\rho_k) = \frac{1}{2}[\| V_o - f(\rho_k) \|_{R_k^{-1}} + \| L(\rho^* - \rho_k) \|_{Q_k^{-1}}] . \tag{13}$$

The first term in the right hand side of Eq. (13) measures the fidelity to the measured data, while the second term measures the fidelity to the *a priori* information. The weighting matrices are selected in manners that are inversely proportional to each variance.

In general, the variance R_k in Eq. (10) is decaying as the iterative mNR-type reconstruction algorithm converges to its real solution. Therefore the weighting matrix for the first term R_k^{-1} need to be increased compared to Q_k^{-1} as the iteration number is increased. To achieve this purpose, we construct the weighting matrices as follows:

$$R_k = Diag[r_k] \quad (\in R^{EP \times EP}) \tag{14}$$

$$Q_k = Diag[q_k] \quad (\in R^{M \times M}) , \tag{15}$$

where,

$$q_k = \beta^{a(K-k+1)} , \tag{16}$$

$$r_k = 1 - q_k . \tag{17}$$

In Eq. (16), a is a scaling factor, $\beta (0 < \beta < 1)$ is forgetting factor, and K is final iteration number.

To find ρ_k which minimizes the augmented cost functional Eq. (13), set the derivative of the cost functional to zero.

$$\Phi_a'(\rho_k) = -[f'(\rho_k)]^T R_k^{-1}[V_o - f(\rho_k)] - L^T Q_k^{-1} L(\rho^* - \rho_k) = 0 \tag{18}$$

The Taylor's series expansion of Φ_a' around ρ_k is expressed by

$$\Phi_a'(\rho_{k+1}) = \Phi_a'(\rho_k) + \Phi_a''(\rho_k)\Delta\rho_k = 0 , \tag{19}$$

where,

$$\Delta\rho_k \equiv \rho_{k+1} - \rho_k , \tag{20}$$

and

$$\Phi_a''(\rho_k) = [f'(\rho_k)]^T R_k^{-1} f'(\rho_k) - [f''(\rho_k)]^T R_k^{-1}[I_M \otimes (V_o - f(\rho_k))] + L^T Q_k^{-1} L \cong [f'(\rho_k)]^T R_k^{-1} f'(\rho_k) + L^T Q_k^{-1} L , \tag{21}$$

where, $\otimes$ stands for Kronecker matrix product.

Therefore, we can obtain the incremental change in resistivity variation as:

$$\Delta\rho_k = -[\Phi_a''(\rho_k)]^{-1}\Phi_a'(\rho_k)$$

$$= \{[f'(\rho_k)]^T R_k^{-1} f'(\rho_k) + L^T Q_k^{-1} L\}^{-1} \cdot \{[f'(\rho_k)]^T R_k^{-1} [V_o - f(\rho_k)] + L^T Q_k^{-1} L(\rho^* - \rho_k)\} \quad (22)$$

In the original mNR algorithm, the information matrix $[f'(\rho_k)]^T f'(\rho_k)$ is often ill conditioned because the ratio of the maximum and minimum eigenvalues of it is very large. But, conditioning of the matrix inside $\{\bullet\}^{-1}$ in the right hand side of Eq. (22) is improved significantly, which helps to stabilize the iterative algorithm. Eqs. (20) and (22) constitutes the iterative update procedure to search the minima of the cost functional Eq. (13). The update procedure of the iterative mNR-type algorithm is continued until it satisfies the stopping performance criterion which is defined in the RMS(root mean square) sense as:

$$\Phi_{ERR}(k) \equiv \sqrt{\frac{[V_o - f(\rho_k)]^T [V_o - f(\rho_k)]}{V_o^T V_o}} \le \varepsilon, \quad (23)$$

where denotes error bound.

III. Simulation results and discussions

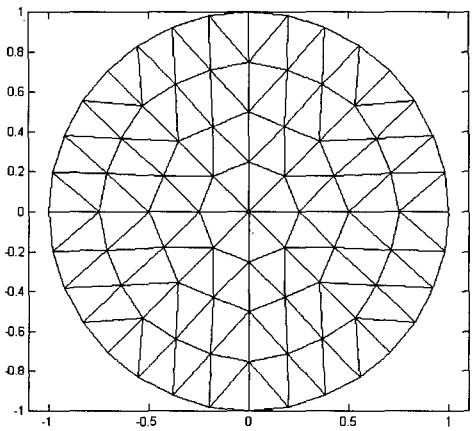

Fig. 1(a) FEM meshes

To illustrate the proposed regularized mNR scheme, we used the FEM meshes with 128 elements(M=128), 81 nodes(N=81) and 32 channels(E=32) as shown in Fig. 1(a). For the true image, we constructed synthetic data with two targets(background conductivity value=0.05 $(\Omega cm)^{-1}$ and target conductivity value=0.005 $(\Omega cm)^{-1}$ so that the contrast ratio is 10:1) as Fig. 1(b).

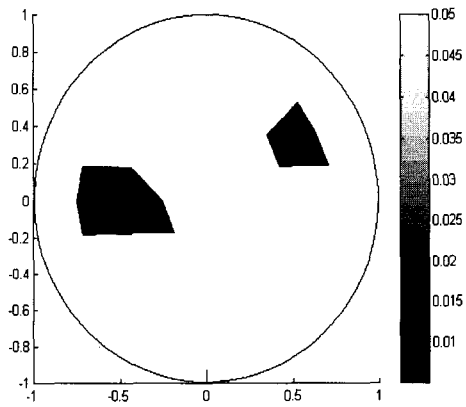

Fig. 1(b) True image

The inverse problem was solved using both the proposed scheme and the conventional regularized mNR to compare the conductivity reconstruction performance. We injected 15 trigonometric current patterns(P=15) and assumed that initial conductivity distribution was the same as background conductivity value. The parameters used in solving the inverse problem are selected as follows; The regularization matrices for both algorithms are set to the same as $L=I_M$, regularization parameter for the conventional regularized mNR is $\alpha_c = 0.1$, scaling factor $\alpha = 0.1$ and forgetting factor $\beta = 0.98$ for the proposed scheme. We selected three cases for the *a priori* information ρ^*; (1) without *a priori* information(that is, ρ^* for both targets are equal to the initial conditions), (2) partial *a priori* information(that is,

ρ^* for left target is set to 20.005 and for right target is equal to the initial condition), and (3) total *a priori* information(that is, ρ^* for both targets are set to 1.50.005).

Fig. 2(a) shows the reconstructed image obtained by the conventional regularized mNR and Figs. 2(b) through (d) are the reconstructed images obtained by the the proposed regularized scheme in cases (1) through (3), respectively after 20 iterations(K=20).

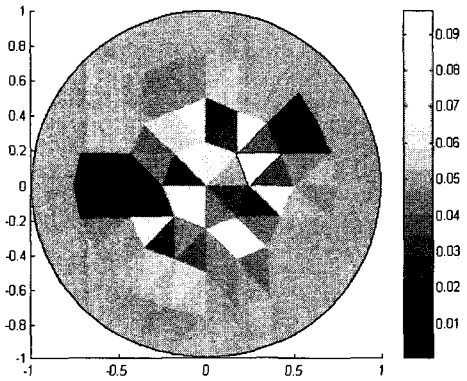

Fig. 2(a) Reconstructed image by the conventional regularized mNR

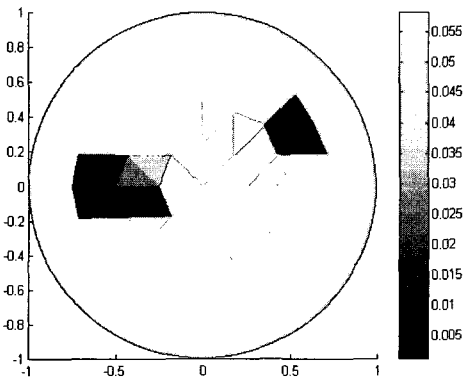

Fig. 2(b) Reconstructed image by the proposed scheme without *a priori* information

As can be seen clearly from these figures, the

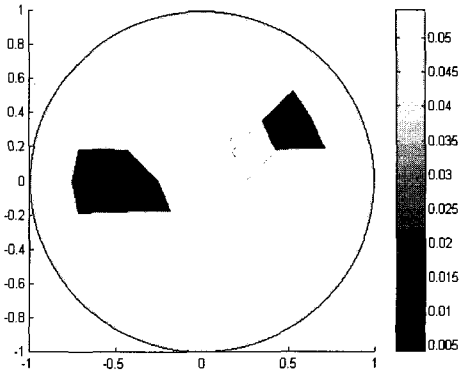

Fig. 2(c) Reconstructed image by the proposed scheme with partial *a priori* information

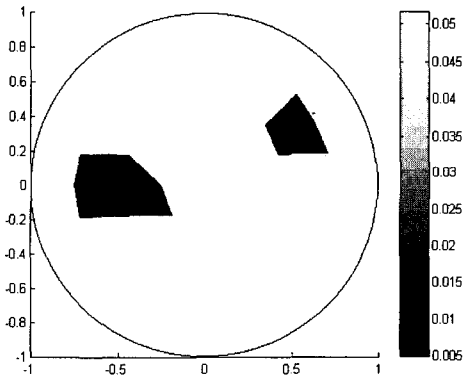

Fig. 2(d) Reconstructed image by the proposed scheme with total *a priori* information

proposed regularized scheme has better reconstruction performance than that of the conventional regularized mNR even in the case without *a priori* information. As can be expected, *a priori* information is closer to the real target values, the proposed scheme has better reconstruction performance. The residual error of the regularized mNR is 8.0908110-6. In addition, the residual errors of the proposed scheme in case (1) through (3) are 1.8355710-6, 8.7354110-8 and 1.22824 10-8, respectively.

Figs. 3(a) and (b) show the convergence of the

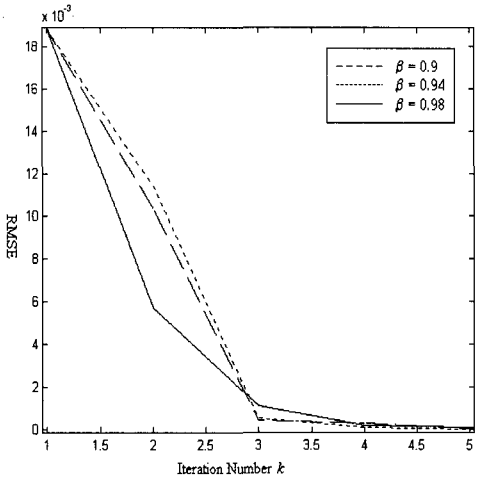

Fig. 3(a) Residual errors in transient period

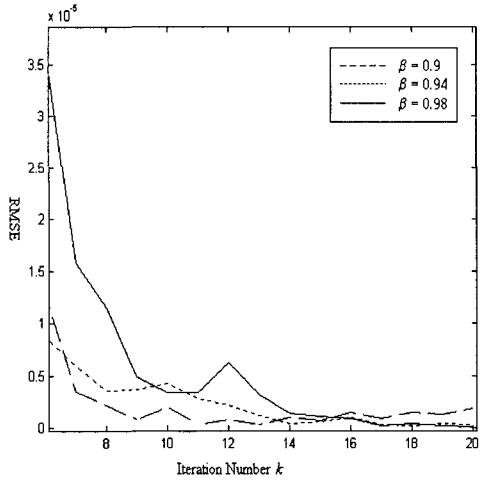

Fig. 3(b) Residual errors in steady-state period

residual errors for the proposed scheme with partial *a priori* information in transient and steady-state period, respectively for different β values. It is noted that large value of β has the small reconstruction error in steady-state. In these simulations, the β values are chosen empirically.

IV. Conclusions

In this paper, we developed a novel regularized mNR scheme for static EIT imaging based on the exponentially weighted least square criterion. The rationale for this paper is that the additional regularization constraint which incorporates *a priori* information into the object functional is helpful to stabilize the mNR reconstruction algorithm only in the transient convergence period. As the iterative mNR-type algorithm converges to its real solution, the ill-conditioning problem becomes less severe. Therefore, in the steady state period, it is desirable to discard the additional constraint to avoid any distortion in final reconstructed image. To accomplish this purpose, exponential weighting matrices are employed to the objective functional, which are functions of the iteration number. Computer simulations using FEM with 32 channels and 128 elements are provided and compared to the conventional regularized mNR algorithm to illustrate the performance of the proposed algorithm. As a result, the proposed regularized scheme has better reconstruction performance than the conventional regularized mNR method at the expense of slightly increased computational burden.

It is supposed that there are many possibilities to improve the performance of the proposed scheme with proper choice of the regularization matrix and the results will be appeared in the sequent paper

Acknowledgement : This work has been carried out under the Nuclear R & D Program by the Ministry of Science and Technology(MOST), Korea

References

[1] J. G. Webster, *Electrical Impedance Tomography*, Adam Hilger, 1990.

[2] J. C. Newell, D. G. Gisser, D. Isaacson, An

Electric Current Tomograph, IEEE Trans. on Biomedical Engineering, vol. 35, no. 10, pp. 828-833, 1987.

[3] M. Cheney, D. Isaacson, J. C. Newell, Electrical Impedance Tomography, SIAM Review, vol. 41, no. 1, pp. 85-101, 1999.

[4] T. J. Yorkey, J. G. Webster, W. J. Tompkins, Comparing Reconstruction Algorithms for Electrical Impedance Tomography, IEEE Trans. on Biomedical Engineering, vol. 34, no. 11, pp. 843-852, 1987.

[5] T. Murai, Y. Kagawa, Electrical Impedance Computed Tomography Based on a Finite Element Model, IEEE Trans. on Biomedical Engineering, vol. 32, no. 3, pp.177-184, 1985.

[6] H. Akaike, A New Look at Statistical Model Identification, IEEE Trans. on Automatic Control, vol. 19, no. 6, pp. 716-723, 1974.

[7] L. Ovacik, Development of an Electrical Impedance Computed Tomographic Two-Phase Flows Analyzer, Final Report, Dept. of Nuclear Engr. and Engr. Physics, Rensselaer Polytechnic Institute, 1998.

[8] C. Cohen-Bacrie, Y. Goussard, R. Guardo, Regularized Reconstruction in Electrical Impedance Tomography Using a Variance Uniformization Constraint, IEEE Trans. on Medical Imaging, vol. 16, no. 5, pp. 170-179, 1997.

[9] M. Vauhkonen, D. Vadasz, P. A. Karjalainen, J. P. Kaipio, Subspace Regularization Method for Electrical Impedance Tomography, 1st International Conference on Bioelectromagnetism, Tampere, Finland, pp. 9-13, 1996.

[10] A. Adler, R. Guardo, Electrical Impedance Tomography: Regularized Imaging and Contrast Detection, IEEE Trans. on Medical Imaging, vol. 15, no. 2, pp. 170-179, 1996.

[11] C. J. Grootveld, A. Segal, B. Scarlett, Regularized Modified Newton-Raphson Technique Applied to Electrical Impedance Tomography, John Wiley & Sons, International Journal of Imaging System Technology, 9, pp. 60-65, 1998.

저 자 소 개

金 慶 淵 (正會員)

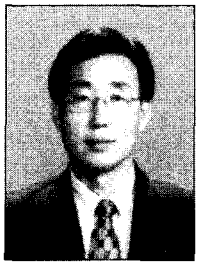

1983년 경북대학교 전자공학과 졸업(학사). 1986년 경북대학교 대학원 잔자공학과 졸업(석사). 1990년 경북대학교 대학원 전자공학과 졸업(공학박사). 1994년-1995년 Univ. of Maryland at Baltimore County Postdoc.. 1990년-현재 제주대학교 전기전자공학부 전임강사/ 조교수/ 부교수. 관심분야 EIT/ ECT, Target Tracking, Data Fusion, Estimation and Identification.

金 奉 奭 (會員申請中)

1999년 제주대학교 전자공학과 졸업(학사). 1999년 - 현재 제주대학교 대학원 전기전자공학과 재학. 관심분야 EIT/ ECT, Kalman Filter Applications